



Effects of composition on the durability and weathering of flat glass

Clarissa Justino de Lima · Brandon Aldinger · Peter de Haan · Telesilla Bristogianni · Fred Veer

Received: 24 January 2022 / Accepted: 19 April 2022

© The Author(s), under exclusive licence to Springer Nature Switzerland AG 2022

Abstract Among the environmental factors affecting glass weathering are humidity, exposure time, temperature, and the presence of pollutants in the atmosphere. Notwithstanding that the weathering produced depends on numerous factors, the important weathering effect of high humidity may be specifically mitigated by using a good chemical composition for the glass. To evaluate this relationship, flat glass samples from three suppliers were studied. The chemical composition of the samples was determined and the variability in compositions was evaluated to verify to what extent these small differences can affect their chemical durability. The chemical durability of the samples was evaluated by determining the hydrolytic resistance of crushed glass powder and using a visual appearance evaluation of bulk samples. The results demonstrate that when the samples are frequently washed, the compositional differences found between the suppliers can cause a significant difference in durability. The samples possessing the highest molar concentrations of Al_2O_3 , and alkaline earth oxides ($\text{MgO} + \text{CaO}$) exhibited the highest

hydrolytic resistance and the least visual deterioration. Differences encountered for the weathering products of glasses of comparable bulk compositions highlight that the process parameters play a major role in the alteration of the surface compositions of the glasses. For the unwashed samples, no consistent correlation was found between hydrolytic resistance and visual deterioration.

Keywords Weathering · Chemical durability · Composition · Flat glass

1 Introduction

1.1 Weathering definition

Glass is regarded as a stable and inert material compared to other materials, such as ceramics and metals; however, when in contact with water in either liquid or vapour phase, it is vulnerable to deterioration. A particular type of surface defect, occasionally found on glass after humidity exposure and temperature variations, is referred to as “weathering”. Visual characteristics of weathering include a greyish appearance, haziness, iridescence, pitting, and different types of crystal formation. Examples of weathered bottles are exhibited in Fig. 1.

Composition changes of multicomponent silicate glasses exposed to the atmosphere, referred to as atmospheric alteration, have been reported for several decades, especially for stained glasses found in the

C. Justino de Lima (✉) · P. de Haan
American Glass Research (Agr) Europe Testing
Laboratory, Delft, The Netherlands
e-mail: cdelima@agrintl.com

B. Aldinger
American Glass Research (Agr) North American Testing
Laboratory, Butler, USA

T. Bristogianni · F. Veer
Faculty of Architecture and Built Environment, Delft, The
Netherlands



Fig. 1 Antique weathered bottles exposed to ambient conditions and their respective sidewalls observed with a digital microscope

windows of European cathedrals. Industrial and cultural heritage curators also have to deal with short-term atmospheric alteration (Alloteau et al. 2017).

It is believed that the rate at which these windows decay has increased substantially during the present century compared to previous centuries. A study was undertaken to investigate the effects of relative humidity (RH) and the presence of airborne pollutants on the rate at which glass decays. Changing the humidity from a dry (15% RH) to a humid environment results in a factor of 10 increase in the hydration rate (Cummings et al. 1998). The results of the same study indicated that environmental pollution with 5 ppm SO₂ or 1 ppm NO₂ does increase the rate at which glass corrodes by a factor of approximately 3 as compared to glass exposed at the same temperature and RH in an ambient of laboratory air. Therefore, RH levels in the environment were found to have a more dramatic effect on the hydration rate than did the levels of SO₂ or NO₂.

Weathering of glass by atmospheric water can be a concern for glass as a building material, as environmental factors can degrade glass strength (Walters and Adams 1975). The reduction in failure strain with weathering time for silicate glasses has been associated with reactions with water that lengthen critical flaws, thereby reducing strength (Ronchetto 2019).

Secondary factors also affect the durability response. Some of these factors are the temperature of the attacking medium, length of contact period, and previous history of the glass, which is related to manufacturing processes like forming method, annealing, special treatments, and storage. Nonetheless, the glass composition is the largest single influence on the chemical durability response (Schaut and Weeks 2017). For this reason, this work aims to determine the relationship between the water resistance and the composition for flat glass obtained from different suppliers. The results can enable a better understanding of the effects of chemical compositional changes and the secondary factors on durability and, therefore, they could prove that the compositional differences found between different commercial glasses could represent a significant difference in the durability of these glasses.

1.2 Weathering mechanism

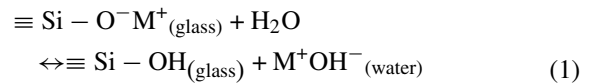
The durability of glass to attack by neutral water can be more difficult to assess than the attack by acid (low

pH) or basic (high pH) solutions because the corrosion mechanism varies with the solution pH. In general, the weathering mechanism of a float glass can be classified into two stages: leaching and dissolution.

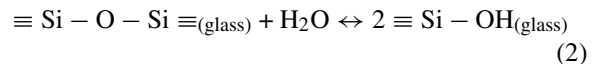
Silicate glasses in acidic environments show mostly incongruent dissolution behavior, releasing elements at different rates. In basic environments, these glasses undergo mostly congruent dissolution, releasing all elements at a single rate as the silica portion of the network is hydrolyzed.

Pure water interacts with glass similarly to a dilute acid, having little effect upon the network formers and intermediates of the glass network while slowly extracting alkali into the solution.

Glasses with modifier cations, such as sodium, undergo exchange reactions where the modifier ions are commonly leached from the glass surface due to reactions with water. This ion exchange process is regarded as the most prevalent initial reaction with alkali-containing glasses like soda-lime-silicate exposed to humid environments. This process can result in the formation of soluble precipitates and is governed by the following reaction (Gösterişlioğlu et al. 2020), in which M represents the alkali ions present in a silicate glass network, such as sodium (Na) or potassium (K):



Because of the low ionic strength of pure water, the release of alkali causes a shift in pH toward basic conditions. If alkali shifts the pH above about pH 9, it catalyzes the hydrolysis of the silicon-oxygen network, breaking the Si–O bonds. This process, which represents the corrosion, can lead to the formation of insoluble precipitates, and is described by the following reaction:



This can lead to an increase in the overall corrosion rate due to the change in mechanism, from the extraction of alkali to congruent dissolution of the complete glass network and all of its constituents into solution (Schaut and Weeks 2017).

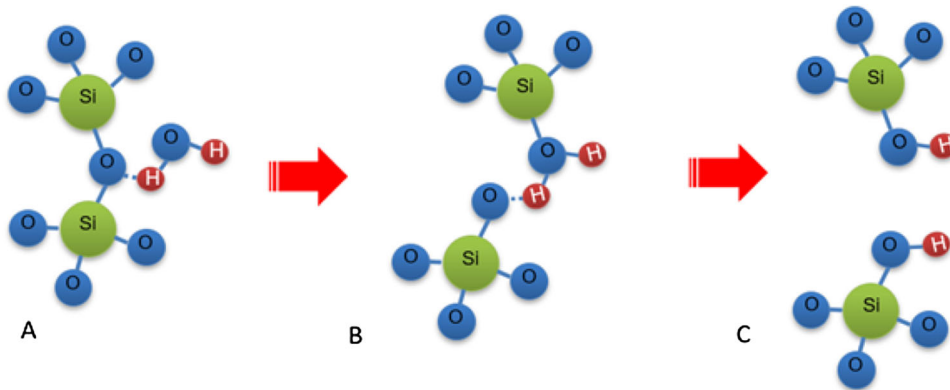


Fig. 2 The stress corrosion mechanism

1.3 Stress corrosion and crack growth

Multiple studies describing the effects of weathering on silicate glasses have been reported, mainly focusing on leaching and layer formation (Cummings et al. 1998), corrosion-induced structural changes (Lombardo et al. 2005) and influence on mechanical performance (Wiederhorn et al. 2013a, b). The stress at a crack tip (σ_{tip}) corresponds to a local peak stress and can be calculated by multiplying the applied or nominal stress ($\sigma_{applied}$), by the stress concentration factor (K_t), as described in the following equation:

$$\sigma_{tip} = \sigma_{applied}(K_t) \quad (3)$$

The stress concentration factor increases with the crack depth (a) and decreases with the crack tip radius of the crack tip (r), as stated by the equation (Schijve 2009):

$$K_t = \left(1 + 2\sqrt{\frac{a}{r}}\right) \quad (4)$$

When an existing flaw in the glass network is exposed to liquid water or atmospheric moisture, the presence of a tensile stress can lead to slow crack growth. The stress corrosion mechanism causes a strength decrease of silicate glasses in the presence of water molecules (Fig. 2a) due to a hydrophilic attack on stretched Si–O–Si bonds (Fig. 2b), which leads to the breakage of these bonds, according to reaction 2, and thus creates an increased opening in the glass (Fig. 2c). Due to this increased opening, the water can penetrate deeper into the glass network and attack the

next bond. As shown in Eq. 4, deeper cracks lead to higher stress concentrations. Therefore, the strength of the glass is not only dependent on the type of surface defect present, but also the duration of the tensile stress and the reaction rate. Consequently, measurements of the durability of glass to attack by water are intrinsically related to the testing conditions, such as time, temperature, and relative humidity.

For a given pre-existing flaw size, there is a minimum applied stress level below which slow crack growth will not occur. In a given environment, the fatigue limit is determined relative to a given initial flaw size, which exists at the beginning of the static fatigue tensile loading interval, and which also has associated with it a specific value of the inert strength (σ_i). The inert strength (σ_i) is the strength measured under conditions when there is no environmental fatigue and, accordingly, must be measured under conditions where the effects of environment-induced reactions are avoided (Kurkjian et al. 2003).

Davis et al. (1983) experimentally determined the existence of the static fatigue limit for mechanically abraded soda-lime-silica glass specimens under constant loading conditions. This threshold level of applied stress has been found to be a constant fraction (0.27) of the inert strength of the pre-existing flaw. This is equivalent to a stress-intensity factor equal to 27 percent of the fracture toughness (K_{IC}) of the glass. The static fatigue limit can be rather expressed in terms of time to failure when the applied stress is equal to the threshold stress level and a static fatigue endurance duration exists at that point.

In contrast, weathering can have a distinct effect on the mechanical properties of glass. Hirao and

Tomozawa (1987) concluded that abraded or indented glasses upon annealing exhibit a strength increase of 20% to 30%. This increase is caused by crack tip blunting, most likely due to viscous flow assisted by water diffused from the atmosphere. Water penetration into fresh fracture surfaces causes the glass just below each surface to swell, increasing its specific volume, and, consequently, forming a local layer of compressive stress at the fracture surface. The local compressive stresses reduce or eliminate the crack-tip stress intensity factor, increasing the resistance of the glass to crack propagation. Accordingly, the glass is stronger and more resistant to failure by static fatigue (Wiederhorn et al. 2013a, b).

1.4 Effects of the tin concentration on weathering

The formation of Si–OH is affected by the tin concentration on the glass surface. Therefore, the weathering in a humid atmosphere has a distinctly different effect on the tin side (bottom face) and the air side (top face) of a float glass (Kolluru et al. 2010).

The phenomenon of bloom, a greyish haze causing a microscopic wrinkling of the surface, is an anomaly occurring at the tin bath side of silicate float glasses and caused by the in-diffusion of tin into the glass melt. This phenomenon is related to the oxidation of Sn^{+2} to Sn^{+4} during reheating of float glasses in air. The Sn^{+4} acts as a network former in the glass structure, changing the glass properties in a superficial layer (Frischat, 2002). Hayashi et al. (2002) reported that the presence of the Sn^{+2} ion on the tin side suppresses the ion exchange reaction between sodium and hydrogen ions on the glass surface. Consequently, the thinner hydrated layer on the tin side can be attributed to the existence of the polarizable Sn^{+2} ion.

The air side exhibits a lower chemical durability as a hydrated layer, developed from the ion exchange reaction between sodium and hydrogen ions, is more easily formed on the air side during weathering. The formation of the hydrated layer depends on the penetration of hydrogen into the glass structure. This hydrated layer on the air-side is thicker and, accordingly, has a lower hardness than the tin side. As a consequence, the air-side surface is less fragile and offers more resistance to crack propagation (Soares et al. 2011). Pisano and Royer-Carfagni (2015) concluded that the distinction between the tin- and the air side may provide a better fit

to the Normal, Log Normal and 2-parameter Weibull distributions. They regressed experimental data according to the 2-parameter Weibull distribution and, using a graphic approach, estimated the 5% fractile of the failure stresses as $\sigma_{5\%} = 54.1$ MPa for the air-side glass-strength, whereas for the tin-side, the 5% fractile ($\sigma_{5\%}$) = 42.87 MPa. Therefore, the difference between the strength of the two glass surfaces cannot be neglected in the definition of the design strength of glass.

2 Experimental

In this work, the durability of the glass samples was measured for crushed glass powder and for bulk samples, and the results of both tests were compared to each other. First, the chemical composition of three samples from different suppliers was measured via X-Ray Fluorescence (XRF). As this work intended to represent commercial glasses and quantify the differences encountered for their compositions, the selected samples originated from three of the largest flat glass manufacturers in the world. Thereafter, three bulk samples from each of the three suppliers were subjected to chemical durability tests and samples in the form of grains were submitted to a hydrolytic resistance test.

2.1 Chemical durability tests using bulk samples

Previous studies indicated that comparing static and cyclic humidity conditions for durability tests using bulk glass samples, considerably more degradation occurred under test protocols using static conditions for some glass compositions, whereas both conditions produced about the same results for others (Walters and Adams 1975). Therefore, the tests performed in this work took place under static humidity conditions.

The samples were stored for 8 weeks in an environmental chamber kept at a temperature of 50 °C and relative humidity of 75%. The pieces of glass were prepared by using a soft cloth, scrubbing first in alcohol, then rinsing well with distilled water, and then they were air-dried. A setup was created hanging the samples with plastic clips on glass rods supported by plastic spacers. Two pieces of each kind of sample were evaluated: one to be washed biweekly with distilled water and one never to be washed for the duration of the

test. The two evaluated samples were biweekly withdrawn from the chamber and the degree of weathering was determined by visually classifying their appearance. Furthermore, one piece was stored in a desiccator and used as a control, and no surface alteration was observed for this piece after eight weeks.

Visual evaluations were made under fluorescent laboratory lighting with a strong white LED lamp while viewing the samples over a black background. The samples were evaluated according to a reference standard (Walters and Adams 1975) and classified into five different conditions:

- A. Excellent: No spots and/or haze are visible when examined with the concentrated beam light source less than 15 cm. from the specimen.
- B. Good: A few spots and/or a slight haze are visible only with lighting conditions as for A.
- C. Fair: Many spots and/or much haze are visible only with lighting conditions as for A.
- D. Poor: Some spots and/or haze are visible without the concentrated beam light source, but with artificial daylight.
- E. Very poor: An excessive accumulation of weathering product is readily visible with artificial daylight.

The last two classifications resulted in an appearance that was judged to be visually unacceptable. For purposes of plotting the data, the appearance classifications were assigned numerical values from 0 to 4 (A = 0 and E = 4).

After 4 weeks of the test and after completing the test, the surfaces of the samples were examined at magnifications up to $100\times$ in an optical microscope to determine the physical nature of the hazy film. The physical characteristics of the film on these samples formed after completing the test were determined at magnifications up to $5500\times$ in a scanning electron microscope (SEM). The elemental composition of the surface features was determined with an energy dispersive X-ray spectrometer (EDX).

2.2 Chemical durability tests using powder samples

The chemical durability tests using glass grains were performed according to USP 43 <660>. In this test, the extraction of grains is performed at 121 °C and followed by the measurement of the degree of the hydrolytic

attack, which is done by the analysis of the extraction solutions. A brief description of the test is provided below.

For each group, the samples to be tested were rinsed with purified water and dried in the oven. At least three of the glass articles were wrapped in clean paper and crushed to produce two samples of about 100 g each in pieces. The glass was crushed and the fragments were transferred to a sieve. The crushing and sieving procedure was repeated until two samples of grains were obtained, each of which weighed more than 10 g. The particle size was between 300 and 425 microns, as collected using sieves. Any iron particles that may be introduced during the crushing, were removed by passing a magnet over them. Each sample was transferred into a beaker for cleaning with acetone and an ultrasonic cleaning operation. The grains were dried and 10 g of the cleaned and dried grains were weighed into two separate conical flasks. Thereafter, 50 mL of carbon dioxide-free purified water were pipetted into each of the conical flasks (test solutions) and 50 mL of carbon dioxide-free purified water was pipetted into a third conical flask that served as a blank. The grains were evenly distributed over the flat bases of the flasks by shaking gently. The three flasks were closed and placed in the autoclave containing water at ambient temperature. It was ensured that they are held above the level of the water in the vessel.

The autoclaving procedure was carried out as indicated in USP <660>, up to a temperature of 121 °C. Thereafter, the hot samples were removed from the autoclave and the flasks were cooled in running tap water as soon as possible, avoiding thermal shock. Thereafter, 0.05 mL of methyl red solution was added to each of the three flasks. The blank solution was immediately titrated with 0.02 M hydrochloric acid, then the test solutions were titrated until the color matched that obtained with the blank solution. The titration volume for the blank solution was subtracted from that for the test solutions. The average value of the results in mL of 0.02 M hydrochloric acid per gram of the sample was calculated. The standard reference material NIST SRM 622 was analyzed along with the samples as a quality assurance standard. The certified value of NIST 622, which is a soda-lime-silica glass, is 7.67 ± 0.38 mL of 0.02 M HCl per 10 g, and the value of NIST 622 measured in the test was 7.79 mL of 0.02 M HCl per 10 g.

Table 1 Normalized chemical composition in weight (wt%) and the global uncertainty of the analysis samples. The molar compositions were calculated based on the chemical compositions in wt%

Compound	Group 1 (wt%)	Group 1 (mol%)	Group 2	Group 2 (mol%)	Group 3	Group 3 (mol%)
SiO ₂	73.35 ± 0.185	72.75	71.51 ± 0.180	70.51	73.37 ± 0.185	72.78
Al ₂ O ₃	0.69 ± 0.015	0.40	1.40 ± 0.030	0.81	0.69 ± 0.015	0.40
Fe ₂ O ₃	0.042 ± 0.004	0.02	0.079 ± 0.008	0.03	0.040 ± 0.004	0.01
CaO	10.26 ± 0.068	10.90	8.90 ± 0.059	9.40	10.25 ± 0.068	10.89
MgO	1.96 ± 0.200	2.90	4.30 ± 0.439	6.32	1.95 ± 0.199	2.88
Na ₂ O	13.18 ± 0.087	12.67	12.87 ± 0.085	12.30	13.16 ± 0.087	12.66
K ₂ O	0.23 ± 0.030	0.15	0.66 ± 0.085	0.42	0.23 ± 0.030	0.15
SO ₃	0.23 ± 0.039	0.17	0.24 ± 0.040	0.18	0.23 ± 0.039	0.17
Others	0.058	0.04	0.041	0.03	0.080	0.06
Total	100.00	100	100.00	100	100.00	100

3 Results

3.1 Chemical composition

Although there are some general industry standard compositions for normal, mid iron and low iron float glass, the actual glass compositions are rarely checked by the end user. A previous study by Veer et al. (2018), reported the chemical composition for multiple samples of one type of bulk glass produced at a single factory at different times. The study indicated that the chemical composition of a single float line is reasonably constant, although there is a clear variation over time.

In this work, three flat glass samples, from three different suppliers, had their compositions determined using XRF. The results are shown in Table 1. Components present in concentrations below 0.05 (in wt%) were omitted from the table. While the composition is reported as fairly constant for a single float line, the variability is higher for different suppliers. The most significant differences were found for the amounts of Al₂O₃, CaO, and MgO.

3.2 Chemical durability- Hydrolytic resistance of glass grains

The results of the hydrolytic tests are shown in Table 2. Group 2 exhibited the highest chemical durability among the three groups. The difference in total alkali

Table 2 Hydrolytic resistance of the samples

Group	Average mL 0.02 M HCL per gram of glass
1	0.83
2	0.67
3	0.82

extracted in the hydrolytic resistance tests for the samples of groups 1 and 3 was minimal, indicating that both groups have a comparable hydrolytic resistance. The estimated error provided by the USP < 660 > method is ± 10% relative and even assuming the maximum possible errors, the resistance of group 2 would be superior to the resistance of the other groups.

3.3 Chemical durability- Visual appearance of bulk samples

Table 3 summarizes the observations regarding the visual appearance of the samples over the 8 week-test. Moreover, during the biweekly control performed at the 4th week, the samples were analyzed with an optical microscope. As can be observed, for groups 1 and 2, only one surface of the unwashed and washed samples exhibited spots and haze. The washed sample of group 3 initially exhibited spots and haze on both surfaces, but after the first biweekly wash, it exhibited these weathering features on only one side. The unwashed sample

Table 3 Summary of weathering observations and haze rating in 75%RH/50°C. The classifications “washed” and “unwashed” refer to biweekly washed and never to be washed samples, respectively. The classifications “one side” and “both sides” indicate if the appearance degradation was observed in one or both surfaces of the sample, respectively

Group	Condition	2 Weeks	4 Weeks	6 Weeks	8 Weeks
1	Washed	B, one side	B, one side	C, one side	C, one side
2	Washed	B, one side	A	B, one side	B, one side
3	Washed	B, both sides	B, one side	C, one side	C, one side
1	Unwashed	B, one side	B, one side	C, one side	C, one side
2	Unwashed	B, one side	B, one side	C, one side	C, one side
3	Unwashed	B, both sides	B, both sides	C, both sides	C, both sides

of the same group exhibited weathering features on its both sides.

The appearance of the unwashed samples after weathering for 4 weeks and 8 weeks and the appearance of the washed samples after 8 weeks is shown in Table 4. The weathering is visible as a whitish haze on the surface. The bright white specks are dust particles loosely adhered to the surface.

Regarding the presence of spots and haze, no significant difference was encountered among the classification of the unwashed samples of the three groups. The samples of the three groups exhibited a fair appearance after the 8 weeks of testing, as shown in Fig. 3.

The effect of the periodic removal of the weathering products was evident for group 2, as shown in Fig. 4. In the 2nd week of the test, the sample exhibited a good condition and was washed. In the 4th week of the test, the appearance of the sample was excellent like at the beginning of the test. After the 8 weeks, the washed sample exhibited a good condition, while the unwashed sample of the same group exhibited a fair condition. For Groups 1 and 3, no significant difference in haze rating was observed between the washed and unwashed samples.

3.4 Microscopy

Microscopy images of the samples of group 1 are shown in Fig. 5.


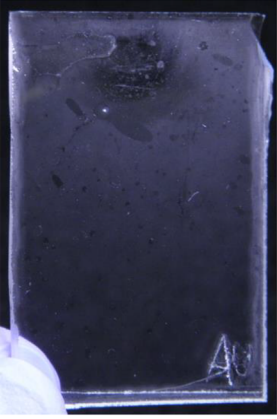
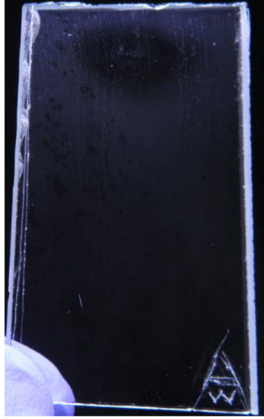

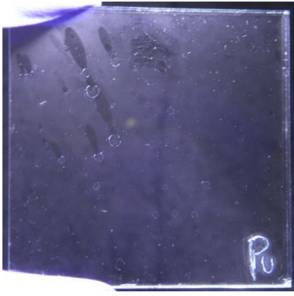
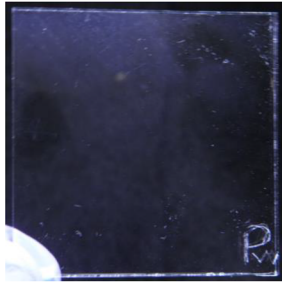

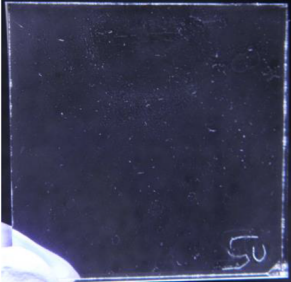

Figure 5b shows the background glass and a crystalline structure. Comparing the signal ratios exhibited in the EDX spectra of the background glass, shown in Fig. 5c, and the crystalline structure, shown in Fig. 5d, the sodium signal increases in the crystalline structure.

Moreover, the carbon signal increases in the spectra of the crystalline structure. Chlorine appears in the spectrum of the crystalline structure, but not for the background glass. As distilled water was used as a source of vapor in the chamber, it is not expected that the chlorine originated from mineral salts in the water but may have originated from residual salts that remained in the chamber after previous experiments using tap water. The compositional analysis of the crystals exhibited in Fig. 5b and e, shown in Table 5, suggests the presence of Na_2CO_3 (sodium carbonate). Furthermore, in Fig. 5b it is possible to notice feathery crystals, which are indicated by yellow arrows, growing out of a thinner layer.

A magnified SEM image of the thinner layer is shown in Fig. 5f. The compositional analysis, shown in Table 5, indicated high molar concentrations of Na and C. Possibly, an altered layer formed, resulting from the dissolution of acidic gases in the atmosphere, such as CO_2 , into the leached surface layer, rich in OH^- and Na^+ ions. Eventually, these gases, as well as particles present in the air, can react with the leached ions originated from the glass. They can form weathering products such as carbonates, sulfates and chlorides on the glass surface (Mendonza Carranza, 2021). This hypothesis could explain the presence of Na_2CO_3 growing out of the layer. However, further investigation is needed to clarify it.

Figure 6 shows microscopy images of the samples of group 2. In contrast with group 1, in which large crystalline deposits were identified, smaller weathering products were found in group 2. A prevailing surface feature, which is shown in Fig. 6a, was identified for this group. This structure exhibited the format of

Table 4 Visual appearance and haze rating of the samples after 4 weeks and 8 weeks of weathering in 75%RH/50°C

Group 1		
		
4 weeks, unwashed samples B, good, one side	8 weeks, unwashed samples C, fair, one side	8 weeks, washed samples C, fair, one side
Group 2		
		
4 weeks, unwashed samples B, good, one side	8 weeks, unwashed samples C, fair, one side	8 weeks, washed samples B, good, one side
Group 3		
		
4 weeks, unwashed samples B, good, both sides	8 weeks, unwashed samples C, fair, both sides	8 weeks, washed samples C, fair, one side

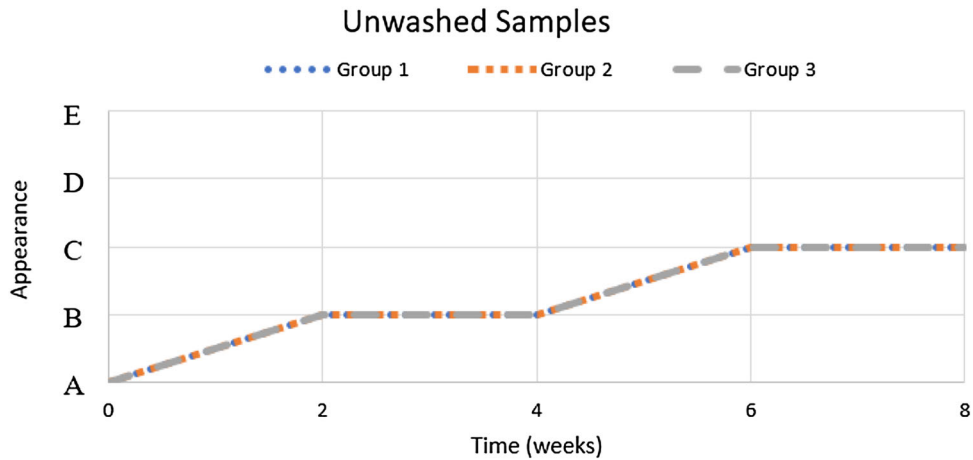


Fig. 3 Visual appearance versus time for unwashed samples

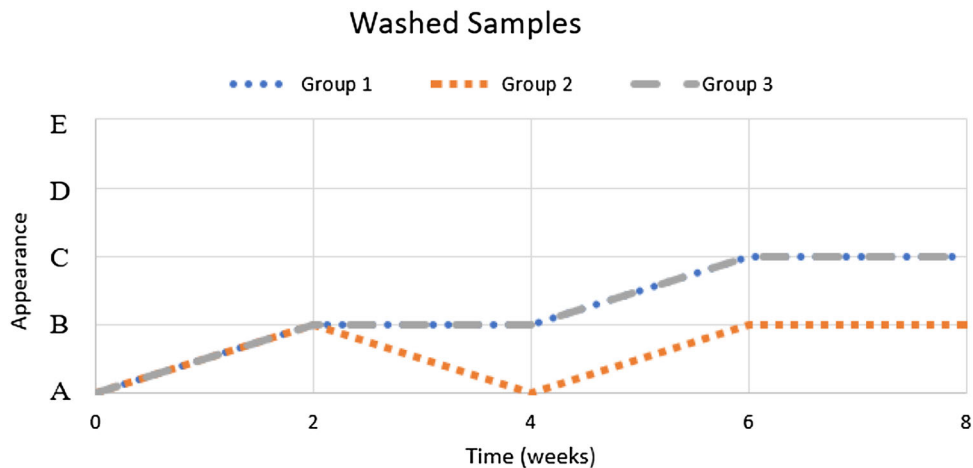


Fig. 4 Visual appearance versus time for washed samples

droplets and an EDX spectrum similar to the altered layer identified in group 1, predominantly with Na, Si, and O, as shown in Fig. 6b. As in group 1, the presence of these elements suggests that the droplets may have been formed through leaching reactions and the presence of Cl suggests the possible formation of salts. These droplets were organized in linear patterns, as shown in Fig. 6c. One possibility is that they could be related to the tin concentration on the glass surface, which is determined by the float process, or related to other stages of the manufacturing processes. However, further research is required to verify the origin of these patterns.

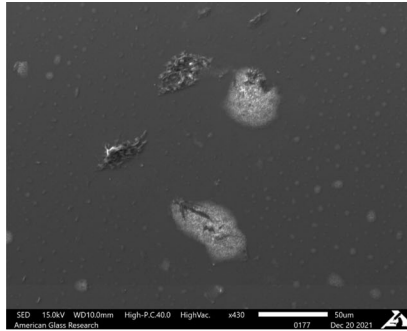
Comparing the unwashed surface, shown in Fig. 6c, and the washed surface, shown in Fig. 6d, it is clear that

for this group the washing process enables significant improvement of the surface condition, removing most of the droplets.

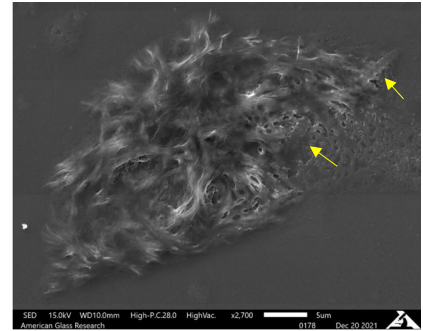
Figure 7 shows microscopy images of the samples of group 3. Especially large geometric crystals of Na_2CO_3 can be found, which are tens of microns long. The surface features identified in pictures Fig. 7a and c are crystals aggregated in long dendritic filaments or in flakes, characteristic of Na_2CO_3 , generally referred to as crow's feet. Their compositions consisted of C, O and Na present in different ratios, as shown in Fig. 7b and d. Moreover, the sodium carbonate crystals were overall more prominent and well-defined in this group than in the others. After washing, most of these dendritic deposits disappeared, as shown in Fig. 7f).

Fig. 5 Scanning electron microscope (SEM) images and EDX analysis of samples from Group 1 weathered for 8 weeks in 75%RH/50 °C. Except for the photo h), all photos are of unwashed samples

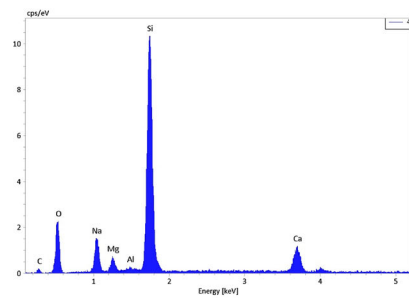
a) Low magnification SEM image of the surface.



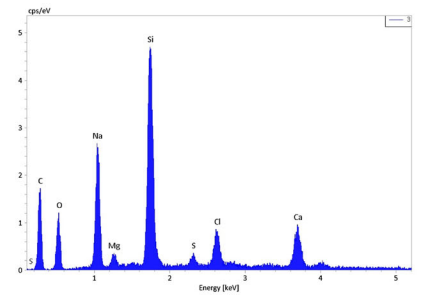
b) Magnified SEM image of a surface feature.



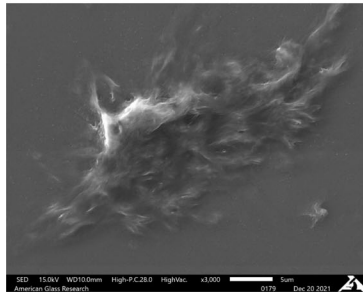
c) EDX spectra of the background glass shown in b).



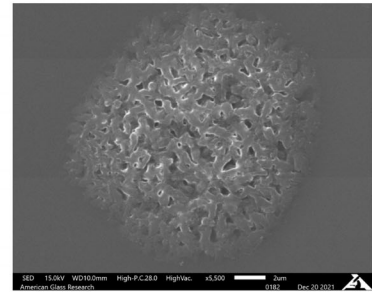
d) EDX spectra of the crystalline structure shown in b).



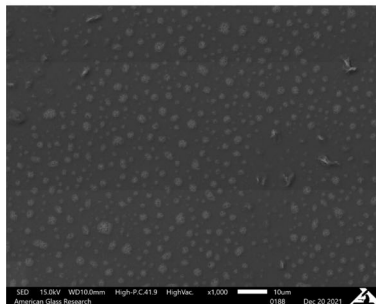
e) Magnified SEM image of a surface feature.



f) Magnified SEM image of a surface feature.



g) Magnified SEM image of unwashed surface.



h) Magnified SEM image of washed surface.

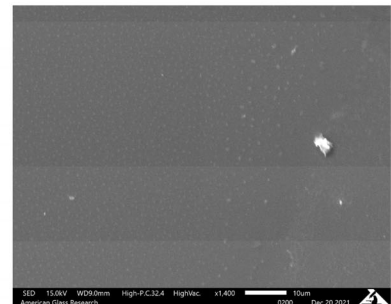
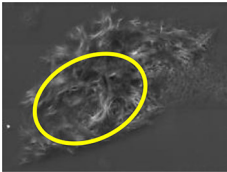
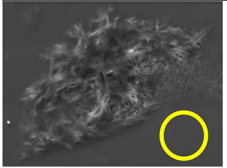
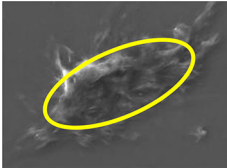
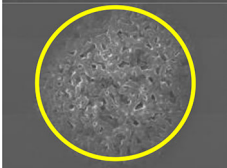


Table 5 EDX spectra compositional percentage determined for crystals, background glass and altered layer of an unwashed sample from group 1. The errors are on the order of 0.5%. However, for these samples, the varied compositions and thicknesses of the weathering crystals would swamp any error inherent to the EDX itself

Figure	Object	Element (mol %)									
		C	O	Na	Mg	Al	Si	S	Cl	Ca	
Fig. 5b		38.31	18.61	14.40	1.27	–	19.63	0.65	2.92	4.20	
Fig. 5b		5.14	31.30	10.11	3.00	0.34	42.64	–	–	7.45	
Fig. 5e		40.53	21.48	15.11	0.82	–	10.56	0.83	7.40	3.27	
Fig. 5f		19.48	24.36	12.14	2.16	–	34.65	–	1.43	5.78	

4 Discussion

The visual analysis represents the most common defect of weathering in real performance. The results of visual analysis of periodically washed samples subjected to a climate test are in good agreement with results obtained from the hydrolytic tests, which indicated that group 2 possesses the highest chemical durability and the chemical durability of group 1 is comparable to group 3. Both methods simulate aging of the glass, however, according to Allsopp et al. (2020), the climate test is more akin to weathering. The superior chemical durability of group 2 can be primarily related to the higher amount of Al_2O_3 in this sample (0.81 mol%) when compared to the samples of group 1 and group 3, both containing 0.40 mol% of Al_2O_3 . Increased alumina contents are associated with their inhibiting effect on the alkaline attack (Bacon 1968), successfully promoting network

connectivity in silicate glasses by eliminating NBOs and tying-up the alkali.

Alkali is the most soluble component of soda-lime glass. A study conducted by Janssens (2013) reported that commercial soda-lime-silica glasses showed preferential leaching of Na compared to K. The amount of total leached alkali turned out to be significantly dependent on the concentration of Al_2O_3 (negative correlation), Na_2O and K_2O (both positive correlation) in the glass. Therefore, both alkali oxides reduce the glass durability, but Na_2O has a greater influence on it. The samples from groups 1 and 3 contained slightly higher amounts of Na_2O (12.60–12.70 mol%) than group 2 (12.30 mol%). Considering the total alkali concentration (sum of Na_2O and K_2O), group 2 has a minimally lower concentration than the other groups (12.82 mol%, 12.72 mol% and 12.81 mol% for groups 1, 2 and 3, respectively). Therefore, it is expected that this negligible variation in alkali concentration does not play a

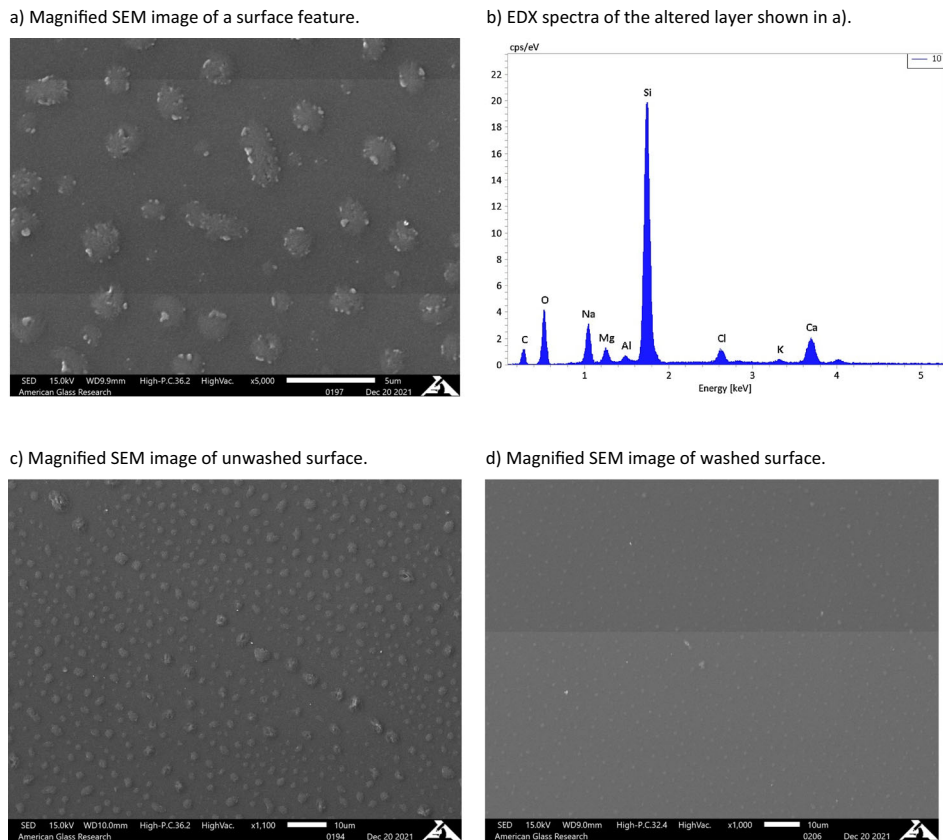


Fig. 6 Scanning electron microscope (SEM) images and EDX analysis of samples from Group 2 weathered for 8 weeks in 75%RH/50 °C. Except for the photo d), all photos are of unwashed samples

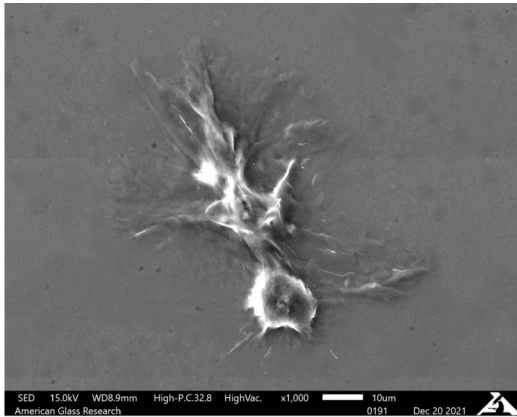
major role in the differences encountered among the chemical durability of the groups.

The alkaline earth ions are relatively less mobile when compared to the alkali. Previous work from Koenderink et al. (2000) investigated the effect of the nature of the alkaline earth cation R (R = Mg, Ca, Sr or Ba) on the durability of soda-lime-silica glasses with molar composition $(\text{RO})_{15}(\text{Na}_2\text{O})_{15}(\text{SiO}_2)_{70}$. The results indicated an enhanced water resistance when going from Ba to Sr to Ca to Mg containing glasses. The results agree with a study that related the thermodynamic hydration energy to the bond energetics of the glass (Jantzen and Plodinec 1984). In this study, the rate of glass dissolution is correlated to the hydration free energy of the glass. A study, from Bacon (1968) corroborated these conclusions, demonstrating that soda-lime glasses containing only MgO are more resistant than those containing only CaO. The samples from groups 1, 2 and 3 contained 2.90 mol%, 6.32 mol%

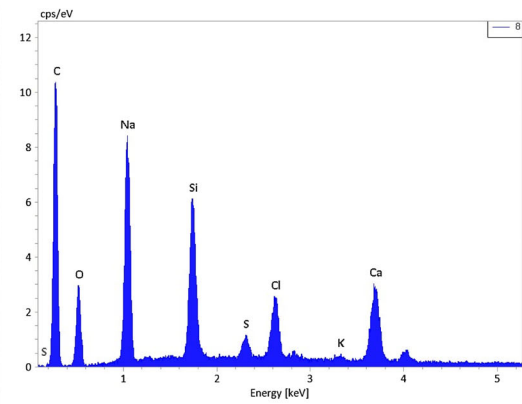
and 2.88 mol% of MgO, respectively. The concentration of alkali earth ions (CaO + MgO) the samples of these same groups was 13.80 mol%, 15.72 mol%, and 13.77 mol%, respectively. Therefore, the higher molar concentration of alkali earth ions and, principally, the significantly larger concentration of MgO in group 2, could have contributed to the higher durability exhibited by the washed samples of this group.

In oxide glasses, where two dissimilar alkali species coexist, the chemical durability can demonstrate remarkable deviation from the linearity when one alkali cation substitutes another at total fixed concentration of alkalis. Similar effects are observed in mixed alkaline-earth glasses. This phenomenon is referred to as mixed alkali effect (Belostotsky 2007). Currently, there are conflicting experimental facts that seem to derail the establishment of empirical rules concerning this effect (Ngai et al. 2002).

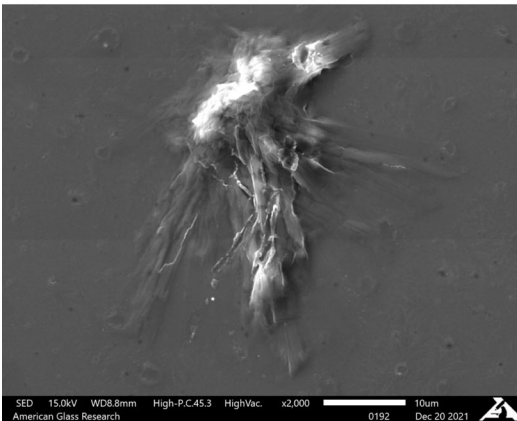
a) Magnified SEM image of a surface feature.



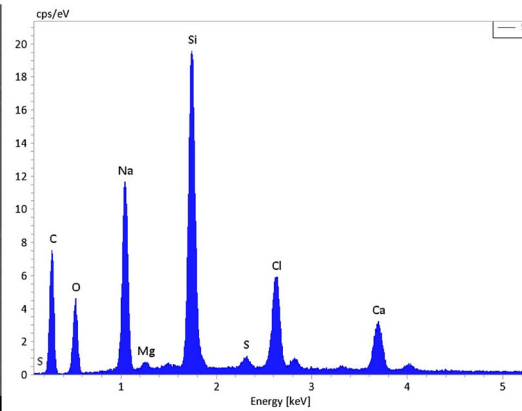
b) EDX spectra of the crystalline structure shown in a).



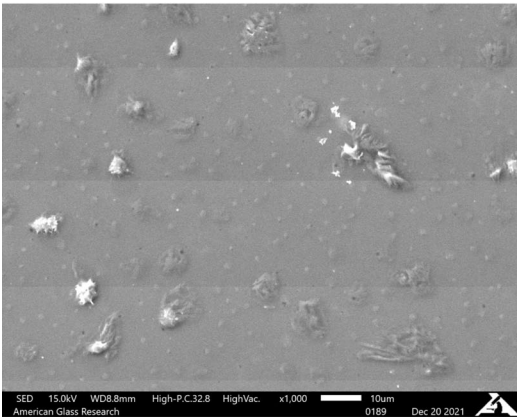
c) Magnified SEM image of a surface feature.



d) EDX spectra of the crystalline structure shown in c).



e) Magnified SEM image of unwashed surface.



f) Magnified SEM image of washed surface.

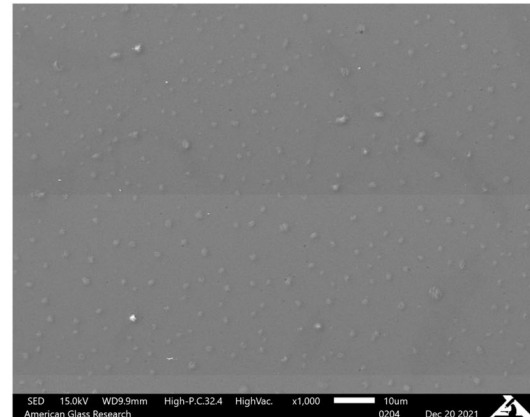


Fig. 7 Scanning electron microscope (SEM) images and EDX analysis of samples from Group 3 weathered for 8 weeks in 75%RH/50 °C. Except for the photo f), all photos are of unwashed samples

Nonetheless, there are two relevant premises reported in literature, which concern alkali, mixed-alkali and mixed alkaline-earth silicate glasses: (i) a SiO₂ content below 66 mol% is mentioned as a threshold below which the chemical durability of glass decreases; and (ii) glasses with CaO contents above 10 mol% are reported as having low chemical resistivity and to deteriorate in high RH environment, or above 12 mol% according to other authors (Rodrigues et al. 2019). This second premise is corroborated by the inferior chemical durability of the samples of groups 1 and 3, which have concentrations of CaO around 10.9 mol%, whereas group 2 has a CaO content of 9.4 mol%.

No consistent correlation was found, however, between the results of the hydrolytic tests and the visual analysis of the unwashed samples. Hydrolytic resistance tests using glass grains determine only the amount of weathering product leached from the glass surface as total weight or as alkali per titration. It is presupposed that the weathering, as measured by these tests, is related to the constituent oxides of the glass on the assumption that it might be an additive property of these components expressed in molar percentages (Owens and Emanuel 1942). On the other hand, the visual inspection of the unwashed samples yielded a qualitative measure of the optical density of the accumulated weathering products. Accordingly, these two tests may not agree because they measure different properties.

Regarding the weathering mechanism, significant differences were observed among the three groups. The weathering can be described by reactions that occur one at a time or simultaneously. The different stages depend on pH variations and were already reported as water adsorption, ion exchange, water molecule hydration to form a thin layer, as well as physical changes resulting from wetting or drying (Tournié et al. 2008). The ion exchange mechanism, described in the introduction, leads to the leaching of sodium to the glass surface. The pH around the reaction sites can change towards a basic environment because of these ion-exchange reactions, accelerating the hydrolysis of siloxane bonds. For group 2, the washing likely resulted in a lower alkalinity of the solution and the diminution of dissolved glass constituents. On the other hand, the poorer visual appearance of the unwashed samples of this group was likely the result of leaching products accumulating and leading to network dissolution.

In humid conditions, the leached ions of a soda-lime silicate glass accumulate on the surface and, as a consequence, react with environmental species to form a wide variety of crystalline deposits on the surface, with sulfates often forming as well (Ronchetto, 2019). In groups 1 and 3, this reaction formed predominantly sodium carbonate. In groups 1 and 2, leaching reactions were also identified, and an altered layer was developed on the glass surface. The compositional analysis of this layer, combined with the high mobility of Na⁺ ions in the glass, suggests a different form of Na₂CO₃. However, a follow-up investigation is suggested to clarify its nature.

Despite the similarity in the compositions of groups 1 and 3, differences were encountered for their weathering products and patterns. Remarkably, the carbonate crystals in group 3 were more prominent and well-defined. Moreover, although remedied by periodically washing, weathering features were observed on both surfaces of the samples of group 3, whereas, under washed and unwashed conditions, they were observed in only one surface of group 1.

These differences indicate that atmospheric glass alteration depends strongly on the glass surface composition. The surface composition may be different from the bulk composition due to process parameters. According to Majéurs et al. (2020), besides the effect of the tin concentration, the presence of SO₂ in the annealing lehr causes surface dealcalization, which can improve the durability of the glass. Additionally, the atmospheric alteration is characterized by its sensitivity to the surface structure and defects, being either compositional gradient, internal stress, scratches, dust and environmental particles, or alteration salts produced in the first alteration stage. During this study, the air side and the tin side were not previously identified and monitored separately during the weathering tests, but studies that investigate the weathering products of each glass surface separately are worth further exploration. Further investigation of the effect of each process parameter on the weathering patterns is also encouraged.

5 Conclusions

A direct relationship between the chemical composition and the amount of weathering was found. Among the three investigated groups, the one that exhibited the highest chemical durability, determined both by

the visual appearance of washed samples and by the hydrolytic test of glass grains, possessed the highest molar concentration of Al_2O_3 , and alkaline earth oxides ($\text{MgO} + \text{CaO}$) in its chemical composition. The SEM/EDX analysis showed that the weathering product was likely formed by an altered layer.

The other two investigated groups, which had a similar chemical composition, exhibited a comparable hydrolytic resistance. The weathering products of both groups were predominantly formed by deposits of Na_2CO_3 . However, variation in the weathering products and patterns were encountered for these groups, indicating that differences in the manufacturing processes of suppliers produce glass surface compositions that diverge significantly from the glass bulk composition.

The slight differences encountered among the chemical compositions of the groups did not have a significant influence on the chemical durability of unwashed samples: after 8 weeks of weathering in 75%RH/50°C, the samples of the three groups had the same haze rating (fair). The results demonstrate the importance of investigating both washed and unwashed samples and looking for a truer representation of the actual surface conditions produced by weathering for predicting product durability. If the samples are frequently washed, weathering could be a less severe problem for some compositions. Therefore, regular window washing could wash away some weathering products and contaminants, avoiding further reactions of the glass surface. However, for most compositions, the washing process did not affect the weathering severity, as it was insufficient to slow down the weathering reactions.

Acknowledgements The authors would like to thank AGR North America testing and analytical laboratories for their support. In particular, we express our gratitude to Gary Smay for the literature recommendation and to Brian Collins for his assistance with the SEM analysis. Neal Nichols and Brian Mitchell are gratefully acknowledged for carrying the hydrolytic resistance tests.

Declarations

Conflict of interest On behalf of all authors, the corresponding author states that there is no conflict of interest.

References

- Alloteau, F., Lehuédé, P., Majéus, O., Biron, I., Dervanian, A., Charpentier, T., Caurant, D.: New insight into atmospheric alteration of alkali-lime silicate glasses. In: *Corrosion Science* 122, pp. 12–25 (2017)
- Allsopp, B.L., Orman, R., Johnson, S.R., Baistow, I., Sanderson, G., Sundberg, P., Stålhandske, C., Grund, L., Andersson, A., Booth, J., Bingham, P.A., Karlsson, S.: Towards improved cover glasses for photovoltaic devices. *Prog. Photovoltaics Res. Appl.* **28**, 1187–1206 (2020)
- Bacon, F.R.: The chemical durability of silicate glass. *Glass Ind.* **49**(8), 438–446 (1968)
- Belostotsky, V.: Defect model for the mixed mobile ion effect. *J Non-Cryst Solids* **353**(11–12), 1078–1090 (2007)
- Cummings, K., Lanford, W.A., Feldmann, M.: Weathering of glass in moist and polluted air. *Nucl. Instrum. Methods Phys. Res. B* **136–138**, 858–862 (1998)
- Davis, M.W., Wasyluk, J.S., Southwick, R.D.: On the static fatigue limit for soda-lime glass. *Glastech. Ber.* **56**(5), 117–124 (1983)
- Frischat, G.H.: Tin ions in float glass cause anomalies. *C. R. Chimie* **5**, 759–763 (2002)
- Gösterişlioğlu, Y.A., Ersundu, A.E., Çelikbilek, E.M., Sökmen, İ.: Investigation the effect of weathering on chemically strengthened flat glasses. *J. Non-Cryst. Solids* **544**, 120192 (2020)
- Hayashi, Y., Fukuda, Y., Kudo, M.: Investigation on changes in surface composition of float glass—mechanisms and effects on the mechanical properties. *Surf. Sci. V* **507–510**, 872–876 (2002)
- Hirao, K., Tomozawa, M.: Kinetics of crack tip blunting of glasses. *J. Am. Ceram. Soc.* **70**, 43–48 (1987)
- Janssens, K.H.A.: *Modern Methods for Analyzing Archaeological and Historical Glass*. Wiley, New York (2013)
- Jantzen, C.M., Plodinec, M.J.: Thermodynamic model of natural, medieval and nuclear waste glass durability. *J. Non-Cryst. Solids* **67**(1–3), 207–223 (1984)
- Koenderink, G.H., Brzesowsky, R.H., Balkenende, A.R.: Effect of the initial stages of leaching on the surface of alkaline earth sodium silicate glasses. *J. Non-Cryst. Solids* **262**, 80–98 (2000)
- Kolluru, P.V., Green, D.J., Pantano, C.H., Muhlstein, C.L.: Effects of surface chemistry on the nanomechanical properties of commercial float glass. *J. Am. Ceram. Soc.* **93**(3), 838–847 (2010)
- Kurkjian, C.R., Gupta, P.K., Brow, R.K., Lower, N.: The intrinsic strength and fatigue of oxide glasses. *J. Non-Cryst. Solids* **316**, 114–124 (2003)
- Lombardo, T., Chabas, A., Lefèvre-A, R., Verità, M., Geotti-Bianchini, F.: Weathering of float glass exposed outdoors in an urban area. *Glas. Technol.* **46**(3), 271–276 (2005)
- Majéus, O., Lehuédé, P., Biron, I., Alloteau, F., Narayanasamy, S., Caurant, D.: Glass alteration in atmospheric conditions: crossing perspectives from cultural heritage, glass industry, and nuclear waste management. *Npj Mater. Degrad.* **4**, 27 (2020)
- Mendonza Carranza, E.K.: Efficiency of cleaning solutions to remove difficult contamination on weathered float glass exposed in an urban environment. Master thesis

- (2021) <https://tesis.pucp.edu.pe/repositorio/handle/20.500.12404/21077>.
- Ngai, K.L., Wang, Y., Moynihan, C.T.: The mixed alkali effect revisited: the importance of ion–ion interactions. *J. Non-Cryst. Solids* **307–310**, 999–1011 (2002)
- Owens, J.S., Emanuel, E.C.: Effect of storage conditions on weathering of commercial glass containers. *J. Am. Ceram. Soc.* **25**(13), 359–371 (1942)
- Pisano, G., Royer-Carfagni, G.: The statistical interpretation of the strength of float glass for structural applications. *Constr. Build. Mater.* **98**, 741–756 (2015)
- Rodrigues, A., Fearn, S., Vilarigues, M.: Mixed reactions: Glass durability and the mixed-alkali effect. *J. Am. Ceram. Soc.* **102**(12), 7278–7287 (2019)
- Ronchetto, E.A.: The effects of fatigue and weathering on the failure behavior of commercial soda-lime silicate glass. Doctoral dissertation 2845 (2019) https://scholarsmine.mst.edu/doctoral_dissertations/2845
- Schaut, R.A., Weeks, W.P.: Historical review of glasses used for parenteral packaging. *PDA J. Pharm. Sci. Technol.* **71**(4), 279–296 (2017)
- Schijve, J. *Fatigue of structures and materials*. Book. ISBN : 978-1-4020-6807-2 (2009)
- Soares, P., Michel, M.D., Mikowski, A., Foerster, C.E., Lepienski, C.M.: Aqueous corrosion of a commercial float glass studied by surface spectroscopies and nanoindentation. *Phys. Chem. Glasses Eur. J. Glass Sci. Technol. B.* **52**(1), 25–30 (2011)
- Tournié, A., Ricciardi, P., Colombari, Ph.: Glass corrosion mechanisms: A multiscale analysis. *Solid State Ion.* **179**, 2142–2154 (2008)
- Veer, F., Bristogianni, T., Justino de Lima, C.: A Re-evaluation of the Physiochemistry of Glass on the Basis of Recent Developments and its Relevance to the Glass Industry. In: *Challenging Glass*. Vol. 6 (2018)
- Walters, H.V., Adams, P.B.: Effects of humidity on the weathering of glass. *J. Non-Cryst. Solids* **19**, 183–199 (1975)
- Wiederhorn, S.M., Fett, T., Rizzi, G., Hoffmann, M.J., Guin, J.: Water penetration—its effect on the strength and toughness of silica glass. *Metall. Mater. Trans. A* **44**(3), 1164–1174 (2013a)
- Wiederhorn, S.M., Fett, T., Rizzi, G., Hoffmann, M.J., Guin, J.P.: The effect of water penetration on crack growth in silica glass. *Eng. Fract. Mech.* **100**, 3–16 (2013b)

Publisher's Note Springer Nature remains neutral with regard to jurisdictional claims in published maps and institutional affiliations.